# Measurement of line overlap for resonant photopumping of transitions in neonlike ions by nickel-like ions

Steven Elliott, Peter Beiersdorfer, and Joseph Nilsen
*University of California, Lawrence Livermore National Laboratory, Livermore, California 94550*
(Received 10 August 1992)

A measurement is made of the $3d$-$4f$ transition energies in the Ni-like ions $Re^{47+}$, $Ir^{49+}$, $Pt^{50+}$, $Au^{51+}$, and $Bi^{55+}$ and the $2p$-$4d$ transition energies in the Ne-like ions $Br^{25+}$, $Kr^{26+}$, $Rb^{27+}$, and $Y^{29+}$ using the Livermore electron-beam ion trap. The ions studied are candidates for an x-ray laser scheme based on resonant photopumping which predicts lasing among the $3p$-$3s$ transitions in a Ne-like ion. The results of the measurements are compared to multiconfiguration Dirac-Fock calculations and systematic differences are found. The best resonance is found for the Pt-Rb pair at 2512 eV, whose energies differ by 0.4±0.1 eV, that is, by only 160 ppm.

PACS number(s): 42.60.By, 32.30.Rj

## INTRODUCTION

The effort to design and build an x-ray laser has been ongoing for quite some time. Several pumping mechanisms have been suggested, including collisional excitation, recombination, photoionization, and photopumping [1]. Of these, only collisional-excitation- and recombination-based schemes have provided gain and lasing. In contrast, the shortest-wavelength photopumped lasing scheme demonstrated to date is 2163 Å [2], though there is evidence of photopumping playing a role in the Ne-like titanium laser at 326.5 Å [3].

The continued interest in photopumping schemes lies in its potential to improve the laser output. It also allows the excitation of lasing transitions not accessible to other mechanisms and thus to test laser kinetics from a different perspective. For example, in collisionally pumped Ne-like x-ray lasers, strong lasing has been observed between the $(2p^{-1}3p)_{J=2}$ upper levels and $(2p^{-1}3s)_{J=1}$ lower levels [4]. (The nomenclature $2p^{-1}$ indicates a vacancy in the closed $2p^6$ shell.) However, lasing between the $(2p^{-1}3p)_{J=0}$ and $(2p^{-1}3s)_{J=1}$ levels is predicted to have the highest gain [5], but is observed to lase only weakly or not at all. The reasons behind the discrepancy between theory and observation are still not understood. Photopumping of the $(2p^{-1}3p)_{J=0}$ level would provide an alternate mechanism to collisional excitation and thus a means to shed new light on the lasing kinetics.

Successful photopumping requires a strong pump line which overlaps with an appropriate absorber line in the lasant. It also requires that the ionization potentials of the pump and lasant ions are comparable so that both coexist under the same plasma conditions. A combination of pump and lasant that meets these requirements is given by high-$Z$ Ni-like and mid-$Z$ Ne-like ions.

Figure 1 shows the basic photopumping laser scheme using the 165-Å (75.1-eV) line in Ne-like Rb as an example. The ground state to $(2p_{1/2}^{-1}4d_{3/2})_{J=1}$ transition in Ne-like Rb is pumped by the emission of the $(3d_{5/2}^{-1}4f_{7/2})_{J=1}$ level in the Ni-like Au ion. Radiative decay of this level feeds the upper level of the lasing transition $(2p_{1/2}^{-1}3p_{1/2})_{J=0}$. The lower laser level then decays back to the ground state. Figure 1 shows the most important radiative rates $\gamma^R$ (in psec$^{-1}$) for producing gain at 165 Å.

Similar resonances are predicted to occur for other close-by Ne-like ions, namely Br, Kr, Sr, and Y, whose $(2p_{1/2}^{-1}4d_{3/2})_{J=1}$ levels may be pumped by the emission of the $(3d_{5/2}^{-1}4f_{7/2})_{J=1}$ level in Ni-like Re, Ir, Tl, and Bi, respectively. In other words, a Ne-like ion with atomic number $Z$ may be pumped by a Ni-like ion with atomic number $(2Z+5)$. We report here the measurement of several of the pairs to determine the feasibility of their use in a photopumping scheme and to provide experimental data for comparison with the theoretical predic-

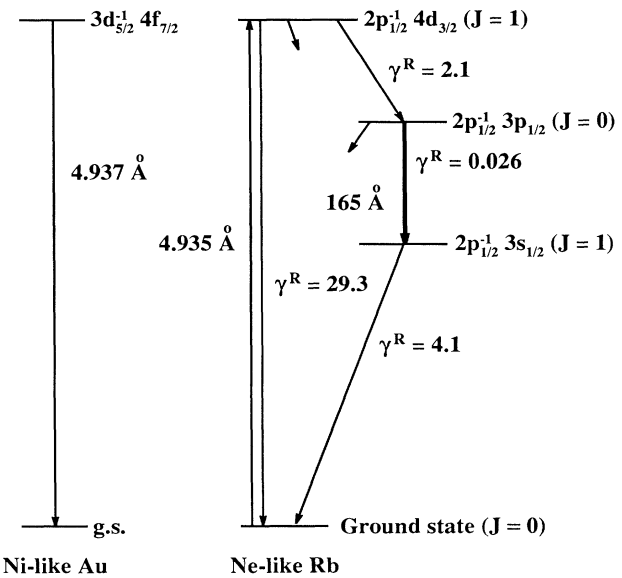


FIG. 1. The level schemes showing the resonant photopumping mechanism using Au-pumped Rb as an example. $\gamma^R$ denotes the radiative transition probability in psec$^{-1}$.

 

TABLE I. The measured and calculated energies (in eV) of the $(3d_{5/2}^{-1}4f_{7/2})_{J=1}$ and $(3d_{3/2}^{-1}4f_{5/2})_{J=1}$ Ni-like lines relative to the Ni-like ground state. The numbers in parentheses represent the uncertainty in the last digit.

| Species | $4f_{7/2}$ Meas. | $4f_{7/2}$ Calc. | $4f_{5/2}$ Meas. | $4f_{5/2}$ Calc. |
|---|---|---|---|---|
| W | | 2111.75 | | 2180.32 |
| Re | 2189.8(4) | 2188.92 | | 2261.06 |
| Os | | 2267.42 | | 2343.31 |
| Ir | 2348.2(5) | 2347.25 | 2425.5(5) | 2427.08 |
| Pt | | 2428.40 | 2511.9(5) | 2512.38 |
| Au | 2511.4(5) | 2510.89 | | 2599.21 |
| Hg | | 2594.78 | | 2687.59 |
| Tl | | 2679.85 | | 2777.52 |
| Pb | | 2766.32 | | 2869.01 |
| Bi | 2854.4(4) | 2854.13 | 2960.8(5) | 2962.07 |

tions of the overlap. Furthermore, for the other Ni-like line $(3d_{3/2}^{-1}4f_{5/2})_{J=1}$ theory predicts a single resonance between Ne-like Rb and Ni-like Pt. That resonance is also measured.

## EXPERIMENT

The electron-beam ion trap (EBIT) at Lawrence Livermore National Laboratory has been described in detail elsewhere [6] and only the salient points will be discussed here. An electron beam ionizes, traps, and excites ions in a 2-cm-long region. The ions are trapped radially by the space charge of the beam. They are trapped axially by electric potentials defined by three collinear cylindrical electrodes through which the beam passes. The middle electrode is held at a slightly lower potential than the other two to define the well. The beam energy is defined by an overall bias of these three electrodes with respect to the electron gun. The charge state of the ion is determined primarily by the electron-beam energy.

The ions are detected by their characteristic x rays emitted after excitation by the beam. For these measurements, the x rays were detected with a flat crystal spectrometer operating in vacuo. The x rays were reflected off either a Ge(111) or a pentaerythritol (PET) (002) crystal and detected in a position-sensitive proportional counter. The wavelength of an x ray seen by the proportional counter is

$$\lambda = 2d \sin[\theta + k(N - N_0)] ,$$

where $N$ is the position in the counter at which the x ray converted, $d$ is the crystal spacing, $\theta$ is the Bragg angle for a calibration line converting at $N_0$, and $k$ is the dispersion determined from the spacing of two calibration lines. The total distance from the EBIT to the crystal and from the crystal to the detector was about 50 cm for the majority of the measurements made here and the resolving power is about 1000. We are able to improve the resolving power to about 2500 by extending the distance between the crystal and the detector and operating the spectrometer in a helium atmosphere. Thus the experiment measured the values in wavelength, and we used $hc = 12\,398.42$ eV Å in the conversion to energy.

We measured five ion pairs, four involving the Ni-like $4f_{7/2}$ level and one involving the Ni-like $4f_{5/2}$ level. For the latter resonance, only the Rb-Pt pair measurement was considered necessary as the other pairs have a large predicted energy difference. For the $4f_{7/2}$ resonance we measured the pairs Br-Re, Kr-Ir, Rb-Au, and Y-Bi. The measurement of the Sr-Tl pair was not attempted due to the handling difficulties of Tl, which is toxic. Tables I and II list the results of the measurements. In addition, any neighboring lines to those of primary interest that were also measured are included in the tables. The energies of the lines were determined relative to hydrogenic and heliumlike reference lines whose energies are theoretically known to a much higher accuracy. In particular, we used transitions from hydrogenlike Al and Si and from He-like ions of S for calibration. The Lyman-$\gamma$ and -$\beta$ transitions in H-like Al were used for the (2000–2200)-eV energy range of the Re-Br pair. The Lyman-$\gamma$ and -$\beta$ transitions in H-like Si were used for the (2350–2550)-eV range of the Rb-Pt-Au and the Kr-Ir lines. The He-like S $K_\beta$ and $K_\gamma$ lines were used for the (2800–3100)-eV region of the Bi-Y lines. The wave-

TABLE II. Measured Ne-like lines energies relative to the Ne-like ground state (eV).

| Ne-like line | Br | Kr | Rb | Y |
|---|---|---|---|---|
| $(2p_{3/2}^{-1}4s_{1/2})_{J=1}$ | 2088.2(5) | | | |
| $(2p_{1/2}^{-1}4s_{1/2})_{J=1}$ | 2136.4(5) | | 2451.6(5) | |
| $(2p_{3/2}^{-1}4d_{5/2})_{J=1}$ | 2144.9(4) | | 2454.0(5) | |
| $(2p_{1/2}^{-1}4d_{3/2})_{J=1}$ | 2191.0(4) | 2349.1(5) | 2512.3(5) | 2857.1(4) |
| $(2s_{1/2}^{-1}4p_{1/2})_{J=1}$ | | | | 3016.3(8) |
| $(2s_{1/2}^{-1}4p_{3/2})_{J=1}$ + $(2p_{3/2}^{-1}5s_{1/2})_{J=1}$ | | | | 3026.1(6) |

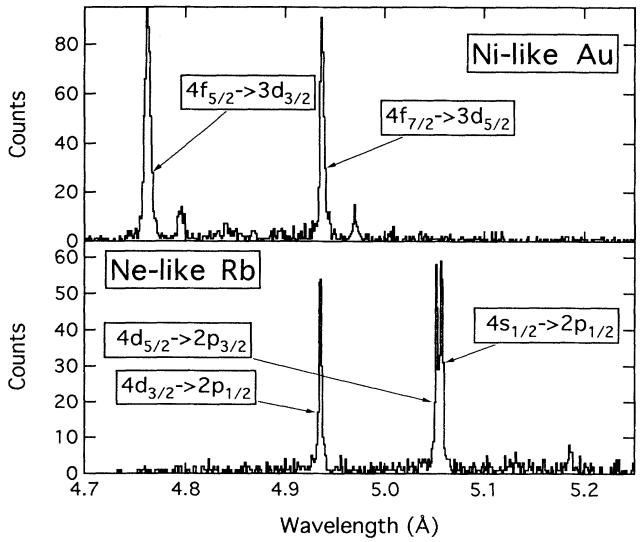


FIG. 2. The spectra of Ni-like Au and Ne-like Rb obtained with a flat crystal spectrometer operating *in vacuo* and employing a Ge(111) crystal. In the measurement, the energy of the electron beam was set to 5 and 3 keV for Au and Rb, respectively.

lengths of the H-like lines were set to the theoretical values quoted by Garcia and Mack [7]; those of the He-like lines were set to the theoretical values quoted by Vainshtein and Safronova [8].

In most of the cases (Re, Ir, Au, Y, Bi, Pt, Al, and Si), the ions were injected into the trap using the metal vacuum vaporization arc source [9]. For the other cases (Rb, S, Br, and Kr) a ballistic gas-injector system [10] was used. The gases vinyl-bromide and krypton served as a source of Br and Kr respectively, and for Rb and S, their high vapor pressures were exploited. Trapped ions are virtually at rest, having a temperature of less than a few hundred eV [10], thus the measurements are not affected by Doppler shifts and the line shapes are purely instrumental. Figure 2 shows representative spectra of $Au^{51+}$ and $Rb^{27+}$.

The uncertainties in the data are a combination of systematic and statistical. The statistical uncertainty was determined by the precision of the location of the line centroids, including those of the calibration lines, and was propagated in quadrature. In addition there was a systematic uncertainty of no larger than 0.3 eV due to the nonlinearity in the proportional counter dispersion. The maximum value of 0.3 eV was added linearly to the statistical uncertainties and the result is the error quoted in Tables I and II for the absolute line energies. We are aware of a previous measurement of the $4f_{7/2}$ line of Ni-like Re at 2189.4(1.9) eV [11]. This value is consistent with ours but of less precision.

## DISCUSSION

For comparison with our measurements, we list the calculated values for the Ni-like and Ne-like transitions in Tables I and III. The line energy predictions are the result of a multiconfiguration Dirac-Fock calculation using the computer code of Grant *et al.* [12] done in the extended-average-level approximation. Systematic differences are found between the calculated and measured energies. The average difference between experiment and theory for the Ne-like $(2p_{1/2}^{-1}4d_{3/2})_{J=1}$ levels is 2.55 eV; that for the Ni-like $(3d_{5/2}^{-1}4f_{7/2})_{J=1}$ level is 0.65 eV.

The uncertainty due to the nonlinearity in the proportional counter dispersion discussed above is the largest contribution to the overall uncertainty; however, it cancels in the difference of nearby lines and thus those uncertainties are smaller. Figure 3 shows a comparison between theory and experiment for the differences in energy between the Ne-like $4d_{3/2}$ and the Ni-like $4f_{7/2}$ ion lines. From Fig. 4, the line overlap is best (0.9 eV) near the Ne-like ions with $Z$ of 36 and 37. That is, for the Kr-Ir and Rb-Au pairs. Explicitly, the results for the energy differences are $\Delta E(\mathrm{Br}(4d_{3/2})\text{-}\mathrm{Re}(4f_{7/2}))=1.2\pm0.15$ eV, $\Delta E(\mathrm{Kr\text{-}Ir})=0.9\pm0.3$ eV, $\Delta E(\mathrm{Rb\text{-}Au})=0.9\pm0.3$ eV, and $\Delta E(\mathrm{Y\text{-}Bi})=2.7\pm0.15$ eV. The figure also shows that once the systematic shifts (1.88 eV) between theoretical and experimental energies have been incorporated in the theory; it reproduces the data well.

Figure 4 shows a comparison between theory and experiment for the differences in energy between the Ne-like $4d_{3/2}$ and the $4f_{5/2}$ Ni-like ion lines. From Fig. 4, the best coincidence occurs for the Ne-like ion with $Z$ of 37, that is, for the Rb-Pt pair. We find that the mismatch of the Rb-Pt pair is yet smaller than that of the Kr-Ir and Rb-Au pairs of Fig. 3 and is a mere $0.4\pm0.2$ eV. Because of the close resonance we remeasured their relative separation with the proportional counter farther away from the crystal to improve the resolution. We obtained the same answer but with a lower uncertainty, $0.4\pm0.1$ eV. Thus the uncertainty for the energy difference of this pair

TABLE III. Calculated Ne-like line energies relative to the Ne-like ground state (eV).

| Ne-like line | Br | Kr | Rb | Sr | Y |
|---|---|---|---|---|---|
| $(2p_{3/2}^{-1}4s_{1/2})_{J=1}$ | 2086.38 | 2235.16 | 2389.01 | 2547.91 | 2711.88 |
| $(2p_{1/2}^{-1}4s_{1/2})_{J=1}$ | 2134.13 | 2289.59 | 2449.81 | 2617.96 | 2790.33 |
| $(2p_{3/2}^{-1}4d_{5/2})_{J=1}$ | 2142.99 | 2294.80 | 2452.40 | 2613.00 | 2780.36 |
| $(2p_{1/2}^{-1}4d_{3/2})_{J=1}$ | 2188.30 | 2346.21 | 2509.92 | 2679.47 | 2854.90 |
| $(2s_{1/2}^{-1}4p_{1/2})_{J=1}$ | 2333.21 | 2496.13 | 2662.71 | 2837.39 | 3017.53 |
| $(2p_{3/2}^{-1}5s_{1/2})_{J=1}$ | 2325.71 | 2492.02 | 2666.17 | 2843.74 | 3026.56 |
| $(2s_{1/2}^{-1}4p_{3/2})_{J=1}$ | 2338.23 | 2501.47 | 2670.55 | 2845.54 | 3027.36 |

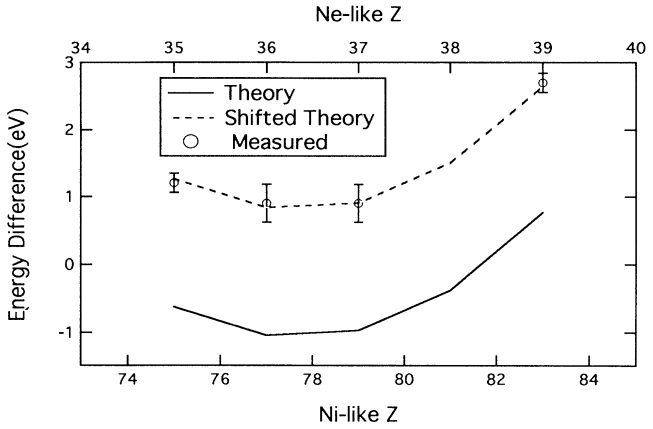


FIG. 3. The comparison of theory and measurement of the energy differences of the Ne-like $(2p_{1/2}^{-1}4d_{3/2})_{J=1}$ lines and Ni-like $(3d_{5/2}^{-1}4f_{7/2})_{J=1}$. The dashed line represents the theoretical predictions shifted by 1.88 eV.

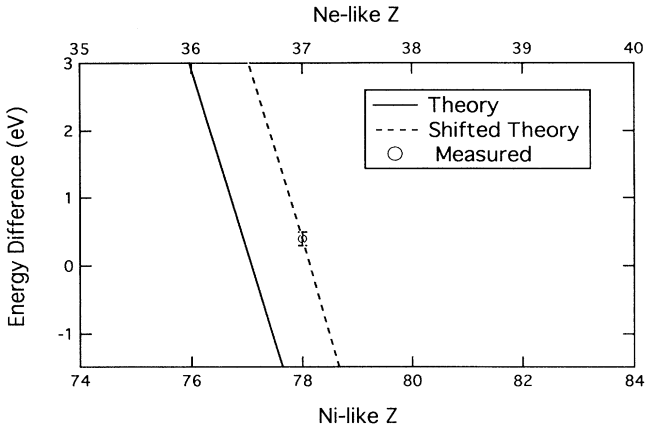


FIG. 4. The comparison of theory and measurement of the energy differences of the Ne-like $(2p_{1/2}^{-1}4d_{3/2})_{J=1}$ lines and Ni-like $(3d_{3/2}^{-1}4f_{5/2})_{J=1}$. The dashed line represents the theoretical predictions shifted by 2.86 eV.

is smaller (by a factor of 2 or better) than the others.

Opacity and Doppler broadening within the laser environment usually determine the degree of overlap required for successful photopumping. The (0.4±0.1)-eV difference between the Rb and Pt lines can be compared to a Doppler broadened linewidth of 0.5-eV full width at half maximum for Rb at a temperature of 500 eV. If the appropriate plasma conditions could be obtained, the $(2p_{1/2}^{-1}3p_{1/2})_{J=0}$ to $(2p_{1/2^{-1}}3s_{1/2})J=1$ transition in Ne-like Rb would lase at 165 Å.

## ACKNOWLEDGMENTS

We thank M. Eckart and A. Hazi for their support. This work was performed under the auspices of the U.S. Department of Energy by Lawrence Livermore National Laboratory under Contract No. W-7405-Eng-48.

[1] R. C. Elton, *X Ray Lasers* (Academic, San Diego, 1990), pp. 99–198.
[2] N. Qi and M. Krishnan, Phys. Rev. Lett. **59**, 2051 (1987).
[3] T. Boehly *et al.*, Phys. Rev. A **42**, 6962 (1990).
[4] D. L. Matthews *et al.*, Phys. Rev. Lett. **54**, 110 (1985); see also Ref. [1].
[5] M. D. Rosen *et al.*, Phys. Rev. Lett. **54**, 106 (1985).
[6] M. A. Levine, R. E. Marrs, J. R. Henderson, D. A. Knapp, and M. B. Schneider, Phys. Scr. **T22**, 157 (1988); R. E. Marrs, M. A. Levine, D. A. Knapp, and J. R. Henderson, Phys. Rev. Lett. **60**, 1715 (1988).
[7] J. D. Garcia and J. E. Mack, J. Opt. Soc. Am. **55**, 654 (1965).
[8] L. A. Vainshtein and U. I. Safronova, Phys. Scr. **31**, 519 (1985).
[9] I. G. Brown, J. E. Galvin, R. A. MacGill, and R. T. Wright, Appl. Phys. Lett. **49**, 1019 (1986).
[10] M. B. Schneider, M. A. Levine, C. L. Bennett, J. R. Henderson, D. A. Knapp, and R. E. Marrs, in *International Symposium on Electron Beam Ion Sources and Their Applications, Upton, NY, 1988,* edited by A. Hershcovitch, AIP Conf. Proc. No. 188 (AIP, New York, 1989), p. 158.
[11] A. Zigler *et al.*, J. Opt. Soc. Am. **70** (1), 129 (1980).
[12] I. P. Grant, B. J. McKenzie, P. H. Norrington, D. F. Mayers, and N. C. Pyper, Comput. Phys. Commun. **21**, 207 (1980).